

Quantitative analyses of calcareous nannoplankton assemblages from the Baden-Sooss section (Middle Miocene of Vienna Basin, Austria)

STJEPAN ČORIĆ¹ and JOHANN HOHENEGGER²

¹Geological Survey of Austria, Neulinggasse 38, A-1030 Vienna, Austria; stjepan.coric@geologie.ac.at

²Institute of Paleontology, Vienna University, Althanstrasse 14, A-1090 Vienna, Austria; johann.hohenegger@univie.ac.at

(Manuscript received December 13, 2007; accepted in revised form June 12, 2008)

Abstract: Quantitative analyses of calcareous nannofossils were carried out on 102 Middle Miocene samples from the scientific borehole at Baden-Sooss (Vienna Basin). All the samples can be assigned to nannoplankton Zone NN5. The content of *Helicosphaera walbersdorffensis* allows correlation with the Mediterranean nannoplankton Subzone MNN5a. Typical near-shore forms such as small reticulofenestrids followed by *Umbilicosphaera jafarii*, *Reticulofenestra haqii*, *Coccolithus pelagicus* and *Reticulofenestra pseudoumbilica* dominate the calcareous nannoplankton assemblages. Inter-species correlations and correlations to stable isotopes and magnetic susceptibility together with multivariate statistical methods (Cluster analysis, Indicator value method, nonmetric Multidimensional Scaling) enabled the reconstruction of trends in the paleoenvironment of the upper water mass during this part of the Badenian. Low variations in abundance of ecologically sensitive species suggest relatively low fluctuating environments. The deeper part of the core (40 to 102 m) shows opposite oscillating trends (with long periods) in salinity and temperature. Around 70 m of the core the salinity maximum is combined with a temperature minimum, while a salinity minimum and temperature maximum can be found around 50 m. Trends in the upper core part are more discontinuous, possibly due to gaps in the sedimentation record caused by intensified tectonics. Generally, a linear trend towards slightly increasing salinity, eutrophication and lowered temperatures could be documented for the upper core part.

Key words: Lower Badenian, Central Paratethys, Vienna Basin, multivariate statistics, calcareous nannofossils, nannoplankton Zone NN5.

Introduction

Detailed investigation of calcareous nannoplankton from the scientific borehole Baden-Sooss was carried out to document the stratigraphic position and paleoecological changes within nannofossil assemblages in Middle Miocene sediments from the southern part of the Vienna Basin (Fig. 1).

The first report about calcareous nannoplankton from the Vienna Basin is from Gümbel (1870). Kamptner (1948) investigated the “Badener Tegel” from the former brickyard at Baden and described 8 new species. He recognized the biostratigraphical and paleoecological importance of this group for Miocene sediments. Further studies were focused on the nannofossil biostratigraphy from different localities in the Austrian part of the Vienna Basin (Fuchs & Stradner 1977; Stradner & Fuchs 1978; Wessely et al. 2007), but they lack, quantitative information, which could lead to a better understanding of the calcareous nannoplankton paleoecology during the Middle Badenian. Numerous publications were dealing with the Miocene stratigraphy and paleoecology from the Mediterranean bioprovince based on quantitative investigations of the calcareous nannoplankton (Fornaciari & Rio 1996; Fornaciari et al. 1996; Sprovieri et al. 2002, etc.). Quantitative analysis allows the identification of events, which can be used for paleoecological interpretation and can be helpful for biostratigraphic correlation.

Calcareous nannoplankton assemblages were newly investigated from the outcrop at the type locality of the Badenian stage, the former brickyard of the Wienerberger Company at Baden-Sooss (Rögl et al. 2008). Biostratigraphic investigation on foraminifera indicates the lower part of the local Upper Lagenidae Zone. The absence of *Helicosphaera ampliaperta* and the presence of *Sphenolithus heteromorphus* in the studied material allow an attribution to the calcareous nannoplankton standard Zone NN5 (Martini 1971). The important short-range species *Helicosphaera waltrans*, occurring in the lowermost part of NN5 could not be identified in the investigated samples. This species was found in the Grund Formation of the Alpine Carpathian Foredeep and in some localities in the Vienna Basin and thus indicates an Early Badenian age corresponding to the Langhian. The borehole Baden-Sooss can be stratigraphically correlated with the overlying interval of *Helicosphaera waltrans* horizon (*Sphenolithus heteromorphus* horizon) described by Švábenická (2002) in the Carpathian Foredeep. According to the biostratigraphic and cyclostratigraphic dating (Hohenegger et al. 2008), this borehole can be positioned between -14.379 and -14.142 Myr, which coincides with the lower part of the *Sphenolithus heteromorphus* Zone (NN5, Martini 1971).

The calcareous nannoplankton as photosynthetic haptophyte algae live in the upper euphotic zone that is directly influenced by ecologic factors such as water temperature, light and inor-

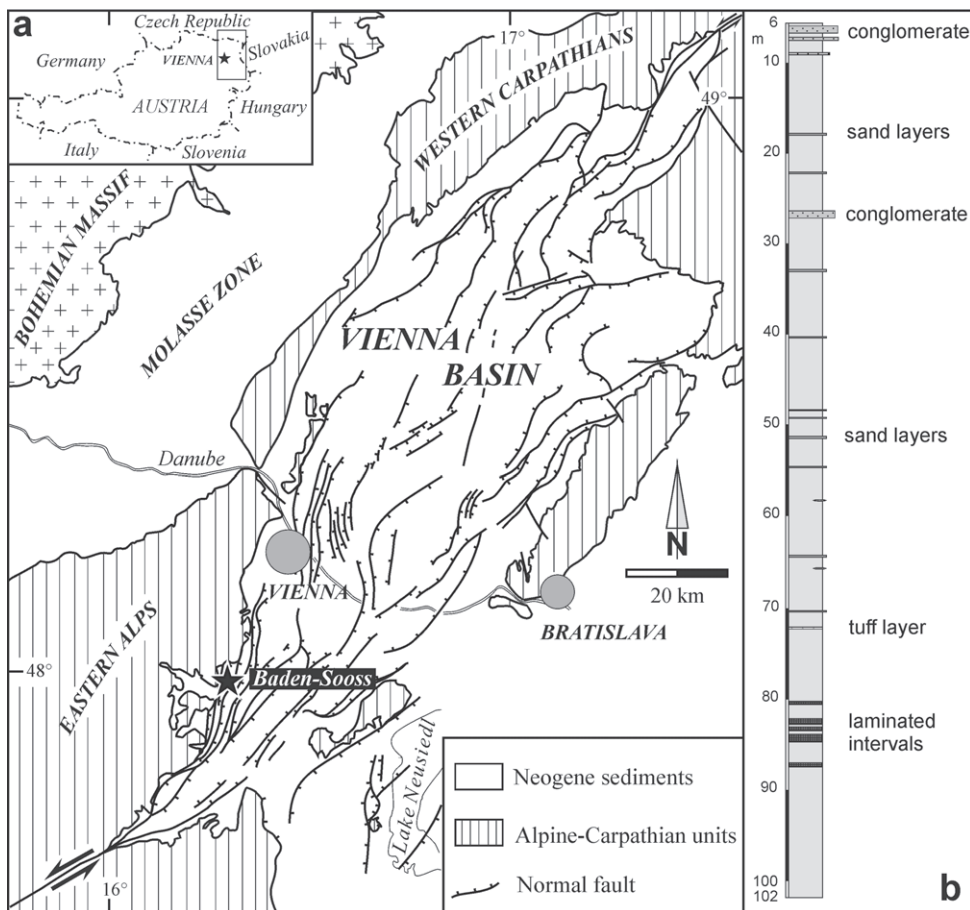


Fig. 1. a — Tectonic map of the Vienna Basin and location of the studied borehole Baden-Sooss. **b** — Schematic sedimentological log of the borehole Baden-Sooss (after Hohenegger et al. 2008).

ganic nutrient supply (nitrate, phosphate, trace elements and vitamins). Generally they flourish in warm, well-stratified, oligotrophic, mid-ocean environments, although numerous species have a broad ecological tolerance (Bown & Young 1998).

Material and methods

The Baden-Sooss scientific borehole penetrates a 102 m succession of intensively bioturbated Middle Miocene sediments at the type locality of the Badenian. The calcareous nannoplankton distribution in this borehole was studied from the whole section (8 m to 101.82 m). Sediments were sampled approximately from each meter, whereas from the lowermost part (100 to 101.82 m) samples were taken at 20 cm intervals.

Smear slides were prepared for all samples using standard procedures and examined under light microscope (cross and parallel nicols) with 1000 \times magnification. In total, 102 samples were analysed.

Quantitative data were obtained according to two methods:

1. counting at least 300 specimens from each smear slide;
2. counting 50 helicoliths from each sample.

A further 100 view squares were checked for important species to interpret the biostratigraphy and paleoecology of the calcareous nannoplankton. Among reticulofenestrids the following species were distinguished: *Reticulofenestra minuta* (reticulofenestrids $< 3 \mu\text{m}$), *R. haqii* (reticulofenestrids 3 to

5 μm), *R. pseudoumbilica* 5 to 7 μm and *R. pseudoumbilica* $> 7 \mu\text{m}$. On the basis of changing abundances of different nannoplankton taxa, the whole section could be subdivided into intervals by eye. For each interval the arithmetical mean and median is given (Tables 1 to 6).

Complex statistical investigations were performed on percentages of the most important and predominating species. For the use of parametrical statistics like the product-moment correlation (Table 9), proportions had to be linearized, whereby the arcsine-root transformation (Linder & Berchthold 1976) was used because of including zero-values. Inter-species correlations and correlations between each species and magnetic susceptibility as well as stable isotopes, obtained from the planktonic foraminifer *Globigerinoides trilobus*, were calculated. Clustering of samples was performed by Ward's method based on standardized Euclidean distances with a subsequent determination of species that is indicative for the obtained clusters (Indicator value method by Dufrene & Legendre 1997). Nonmetrical Multidimensional Scaling (nMDS), also based on standardized Euclidean distances, was used for the representation of relations between samples and species in a low-dimensional space. The grade of changes in floral composition along the core could be measured as distances between subsequent samples in the low dimensional character space gained by nMDS. Large distances indicate a strong turnover in floral composition and longer intervals of large distances are typical for intensive environmental oscillations.

The basic lists can be found as an Electronic Supplement of this paper in web version at <http://www.geologicacarpathica.sk>. Simple statistical analyses were calculated with EXCEL, while for complex analyses the program packages SPSS (2006) and PC-ORD (McCune & Mefford 1999) were used.

Results

Middle Miocene sediments from the Baden-Sooss core generally contain very well-preserved and common calcareous nannoplankton assemblages (Fig. 2). All assemblages are dominated by *Reticulofenestra minuta*. *Coccolithus pelagicus*, helicoliths, *Reticulofenestra gelida*, *R. haqii*, *R. pseudoumbilica*, and *Umbilicosphaera jafarii* occur less frequently, but regularly and continually. *Helicosphaera cartieri* and *H. walbersdorffensis* occur regularly among helicoliths, whereas *H. euphratis*, *H. minuta* and *H. wallichii* are relatively rare. Rare but relatively continual are *Acanthoica cohenii*, *Braarudosphaera bigelowii*, *Coccolithus miopelagicus*, *Coronocyclus nitescens*, *Coronosphaera mediterranea*, *Criptococcolithus mediaperforatus*, *Cyclicarololithus floridanus*, *Geminilithella rotula*, *Hayella chalangeri*, *Holodiscolithus macroporus*, *Micrantholithus vesper*, *Pontosphaera multipora*, *Rhabdosphaera sicca*, *Sphenolithus heteromorphus* and *Sphenolithus moriformis*. Rare and irregularly found are *Calcidiscus leptoporus*, *C. premacintyrei*, *C. tropicus*, *Calciosolenia murrayi*, *Ilselithina fusa*, *Microcrantolithus articulatus*, *Perforocalcinella fusiformis*, *Pontosphaera discopora*, *Syracosphaera pulchra*, *Thoracosphaera heimii*, *Th. saxeae* and *Triquetrorhabdulus milowii*.

The distribution of autochthonous and reworked calcareous nannofossils in the borehole Baden-Sooss is alphabetically arranged and listed in Table 7 (autochthonous nannofossils) and Table 8a,b (reworked nannofossils).

Species distribution

Coccolithus pelagicus

The abundance pattern of *C. pelagicus* (Fig. 3a) shows 6 distinct periods with abundance fluctuations. Abundances of *C. pelagicus* vary between 0 and 9.7 % in intervals 2, 4 and 6 and are thus negatively correlated with magnetic susceptibility (Fig. 3a, Table 9). *Coccolithus pelagicus* shows higher percentages in intervals 1, 3 and 5. They oscillate here between 0.9 % and 16 % getting maximum values in the upper part of the core (interval 5). These intervals can be correlated with lower values of magnetic susceptibility. Beside the negative correlation of *C. pelagicus* to magnetic susceptibility, this species is also negatively correlated with *R. minuta*, but significant positively correlated with *R. haqii* and the reworked nannoplankton (Table 9).

Reticulofenestra pseudoumbilica

Fornaciari et al. (1996, 1997) showed that *R. pseudoumbilica* with a diameter of 5 to 7 μm commonly occurs within the NN5 nannoplankton Zone of the Mediterranean region. They used

the first common occurrence (FCO) of larger *R. pseudoumbilica* (with diameter > 7 μm) for subdividing the nannoplankton Zone MNN6 into Subzones MNN6a and MNN6b.

Sediments from Baden-Sooss contain a very few larger *R. pseudoumbilica* and therefore they were combined with the smaller species. According to the abundance pattern of *R. pseudoumbilica*, the borehole Baden-Sooss can be subdivided into three intervals (Fig. 3b, Table 2). Intervals 1 (mean 4.87, median 4.61) and 3 (mean 2.66, median 2.50) contain lower percentages of *R. pseudoumbilica* with values between 0 % and 8.8 %. Additionally, interval 3 can be subdivided into 4 subunits: 3A and 3C are characterized by lower and 3B and 3D by higher concentrations of *R. pseudoumbilica*. The interval 2 (from 55.0 m to 80.02 m) contains samples with higher percentages of *R. pseudoumbilica* between 4.8 and 19.4 % (mean 9.29 %, median 8.74 %). This species is negatively correlated with *R. minuta* and shows a single but insignificant positive correlation to *U. jafarii* (Table 9).

Reticulofenestra minuta

Reticulofenestra minuta and *R. haqii* dominate in the Baden-Sooss core, with participation in nannoplankton assemblages between 44.7 and 94.1 %. On the basis of variation in the content of small reticulofenestrids, the scientific borehole at Baden-Sooss can be subdivided into six intervals (Fig. 3c, Table 3). Samples from intervals 2, 4 and 6 contain lower numbers of small reticulofenestrids, which vary between 41.4 and 74.2 %. Intervals 1, 3 and 5 contain increased percentages of *R. minuta* oscillating between 46.6 % and 89 %. *Reticulofenestra minuta* is significantly negatively correlated with all other species (except *H. walbersdorffensis*) and the reworked nannoplankton (Table 9). Peaks in the abundance of *R. haqii* (Fig. 3d) coincide with maximum values of magnetic susceptibility.

Umbilicosphaera jafarii

On the basis of the abundance of *U. jafarii*, six intervals can be distinguished in the Baden-Sooss core (Fig. 3e, Table 4). Intervals 1, 4 and 6 contain lower percentages (0 to 13.8 %), whereas intervals 3 and 5 are characterized by a higher amount (1.9 to 29.3 %). *Umbilicosphaera jafarii* increases gradually in interval 2 from 1.9 % to 12.5 %. An extremely significant negative correlation could be observed between *U. jafarii* and *R. minuta* (Table 9).

Sphenolithus heteromorphus

Sphenoliths are represented by *Sphenolithus heteromorphus*, *S. milanetti* and *S. moriformis*. The biostratigraphically important species *S. heteromorphus* is scarce and varies from 0 to 3.58 %. This species was not observed in the interval from 51.0 to 59.02 m. Figure 3f illustrates the abundance pattern of *S. heteromorphus* and *S. moriformis* in the core. Both species demonstrate similar changes in their abundances. Intervals 1, 4 and 6 contain lower concentrations of sphenoliths, which vary from 0 to 1.3 % (Table 5). Percentages of *S. heteromorphus* and *S. moriformis* increased in the interval 6 from 8

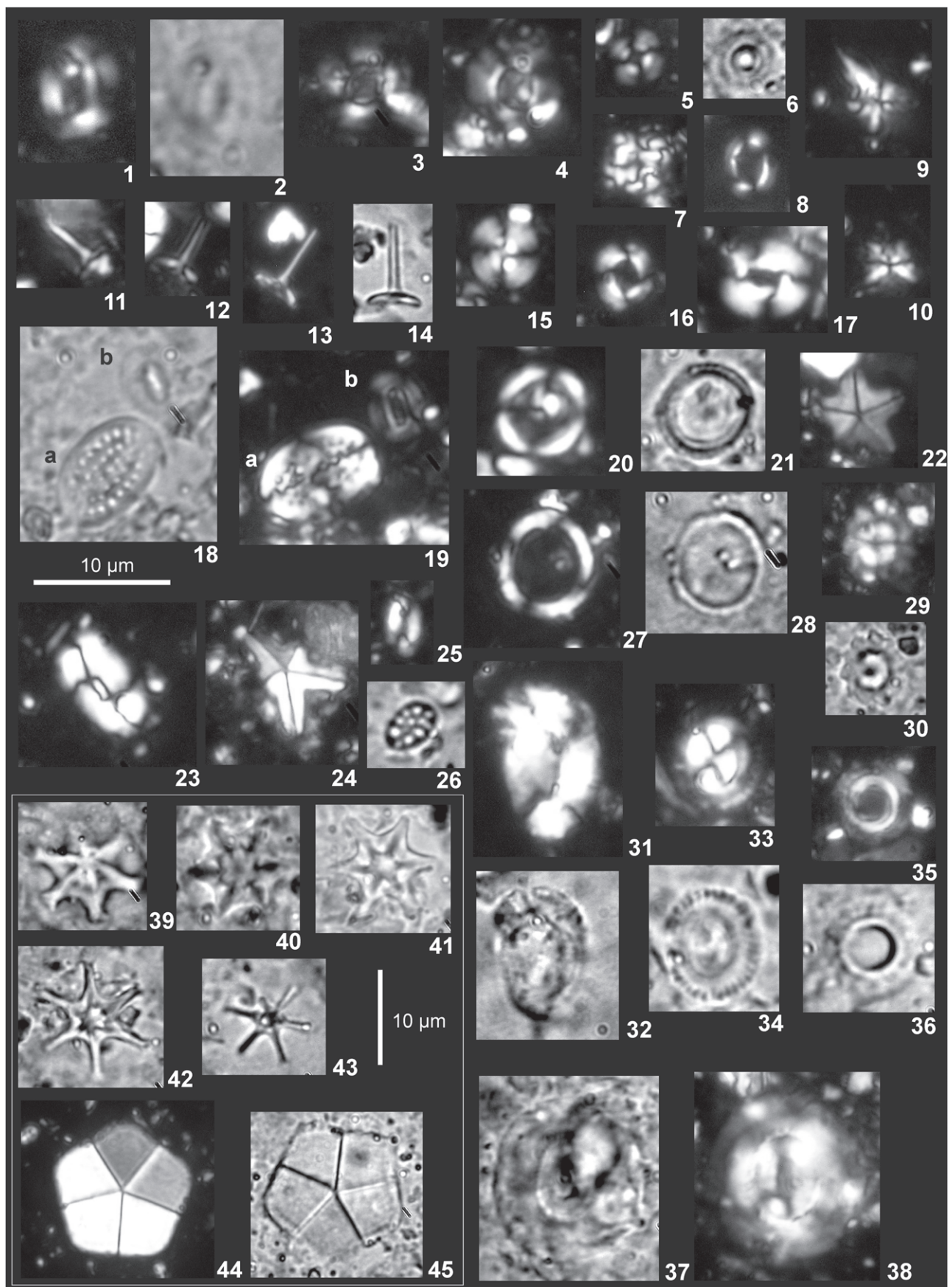


Fig. 2.

to 31.2 m. *Sphenolithus heteromorphus* was not observed in interval 4. Intervals 2 and 5 are characterized by the highest percentages of sphenoliths with maximum values of 2.9 % in interval 2 and 4.2 % in interval 5. A stepwise decrease from 1.6 to 0 % was noted in interval 3. Maximal abundances of sphenoliths can be correlated with highest values of magnetic susceptibility, which is also expressed in the high positive correlation (Table 9). Lower, but still significant correlations are found between *S. heteromorphus* and *R. haqii* (positively correlated) and between *S. heteromorphus* and *R. minuta* (negatively correlated; Table 9).

Helicoliths

In the Baden-Sooss core, *Helicosphaera carteri* and *H. walbersdorfensis* occur regularly but in low percentages. *Helicosphaera carteri* (Fig. 3h), a cosmopolitan species, occurs in low percentages from 0 to 5.8 % (in sample 34.0 to 34.02 m). A slight enrichment of this species in three intervals (from 72.00 to 77.02 m, 33.2 to 36.02 m and from 8 to 17.23 m) is remarkable. *Helicosphaera walbersdorfensis*, a small form, which decreases in abundance along the core is used to define the Middle Miocene MNN5a/MNN5b Sub-zones in the Mediterranean region (Fornaciari et al. 1996). Samples from Baden-Sooss contain low percentages with higher proportions in the lowermost part of the core showing a maximum of 14.5 % in sample 100.80–100.83 m. *Helicosphaera walbersdorfensis* is replaced by *H. carteri*, which shows increasing values within the counted 50 helicoliths (Fig. 3g) that can be correlated with higher magnetic susceptibility. This replacement is also found in the significant negative correlation between the two helicolith species (Table 9).

Reworking

Reworked specimens were counted through the borehole Baden-Sooss and alphabetically listed in Table 2. They are represented by the Late Cretaceous taxa *Arkhangelskiella cymbiformis*, *A. maastrichtiana*, *Biscutum ellipticum*, *Brownsonia parka constricta*, *Watznaueria barnesae* etc. Reworked

Paleogene to Early Miocene specimens are more common: *Chiasmolithus grandis*, *Discoaster kuepperi*, *D. lodoensis*, *D. multiradiatus*, *Ericsonia formosa*, *Helicosphaera mediterranea*, *Reticulofenestra bisecta*, *R. dictyoda*, *Sphenolithus radians*, *Toweius* spp., *Zygrhablithus bijugatus* etc.

Different concentrations of reworked taxa allow us to distinguish six intervals in the Baden-Sooss core (Fig. 3j, Table 6): intervals 2, 4 and 6 with higher percentages and intervals 1, 3 and 5 with lower percentages. The intervals can be positively correlated with magnetic susceptibility. Especially higher percentages of reworking in interval 6 and the prominent peak in interval 5 (sample 22.00–22.03 m) indicate higher tectonic activity.

Discoasterids

Discoasterids are well preserved, but they occur sporadically in very low percentages, which do not exceed 1.86 % (Sample 10.00–10.03 m). They are represented by *Discoaster adamanteus*, *D. deflandrei*, *D. exilis*, *D. formosus*, *D. musicus*, *D. sanmiguelensis*, *D. variabilis* and *Discoaster* sp.

Multivariate analyses

Cluster analysis by Ward's method differentiated 4 clusters (Fig. 4). All characteristic species are present in **Cluster 1** demonstrating high indicator values (IV) from 15 to 32 (Table 10). The most significant species are *Reticulofenestra haqii* (IV 32) and *Helicosphaera walbersdorfensis* (IV 30) followed after a gap by *R. minuta* (IV 26). The central position of Cluster 1 within the remaining classes is demonstrated by nMDS (Fig. 5), where samples belonging to Cluster 1 intermingle with Cluster 2, while the broad contact to Cluster 1 and the narrow contact to Cluster 3 are contiguous.

Therefore, the separation of **Cluster 2** from the former is artificial caused by the necessity of creating distinct classes in hierarchical classification (Fig. 4). Nevertheless, the second cluster differs from the former in two respects. First, a single species (*R. minuta*) has as indicator values (IV 29) distinctly higher than in other species; second, *Sphenolithus heteromorphus* is extremely rare. In nMDS, samples belonging to this cluster are lo-

-
- Fig. 2. 1–2** — *Cryptococcoolithus mediaperforatus* (Varol, 1991) de Kaenel & Villa, 1996. Sample 54.00–54.02 m. **3** — *Hayella challengerii* (Müller, 1974) Theodoridis, 1984. Sample 39.20–39.22 m. **4** — *Hughesiella tasmaniae* (Edwards & Perch-Nielsen, 1975) de Kaenel & Villa, 1996. Sample 39.20–39.22 m. **5, 6** — *Umbilicosphaera jafarii* Müller, 1974. Sample 39.20–39.22 m. **7** — *Reticulofenestra minuta* Roth, 1970. Sample 99.00–99.02 m. **8, 16** — *Reticulofenestra pseudoumbilica* (Gartner, 1967) Gartner, 1969. Sample 99.00–99.02 m. **9, 10** — *Sphenolithus heteromorphus* Deflandre, 1953. Sample 39.20–39.22 m. **11** — *Rhabdosphaera clavigera* Murray & Blackman, 1898. Sample 36.00–36.02 m. **12–14** — *Rhabdosphaera sicca* Stradner, 1963. Sample 78.00–78.02 m. **15** — *Cyclicargolithus floridanus* (Roth & Hay, 1967) Bukry, 1971. Sample 36.00–36.02 m. **17** — *Reticulofenestra gelida* (Geitzenauer, 1972) Backman, 1978. Sample 99.00–99.02 m. **18, 19** — a — *Pontosphaera multipora* (Kamptner, 1948) Roth, 1970; b — *Cryptococcoolithus mediaperforatus* (Varol, 1991) de Kaenel & Villa, 1996. Sample 78.00–78.02 m. **20, 21, 27, 28** — *Coronocyclus nitescens* (Kamptner, 1963) Bramlette & Wilcoxon, 1967. Sample 69.20–30.22 m. **22** — *Micrantholithus flos* Deflandre, 1950. Sample 99.00–99.02 m. **23** — *Helicosphaera euphratis* Haq, 1966. Sample 39.20–39.22 m. **24** — *Micrantholithus* sp. Sample 99.00–99.02 m. **25** — *Helicosphaera walbersdorfensis* Müller, 1974. Sample 99.00–99.02 m. **26** — *Holodiscolithus macroporus* (Deflandre, 1954) Roth, 1970. Sample 60.00–60.02 m. **29, 30** — *Discoaster kuepperi* Stradner, 1959. Sample 99.00–99.02 m. **31, 32** — *Helicosphaera carteri* (Wallich, 1877) Kamptner, 1954. Sample 99.00–99.02 m. **33, 34** — *Coccolithus pelagicus* (Wallich, 1871) Schiller, 1930. Sample 60.00–60.02 m. **35, 36** — *Geminilithella rotula* Kamptner, 1956. Sample 60.00–60.02 m. **37, 38** — *Coccolithus miopelagicus* Bukry, 1971. Sample 60.00–60.02 m. **39–41** — *Discoaster sanmiguelensis* Bukry, 1981. Sample 60.00–60.02 m. **42** — *Discoaster variabilis* Martini & Bramlette, 1963. Sample 60.00–60.02 m. **43** — *Discoaster exilis* Martini & Bramlette, 1963. Sample 60.00–60.02 m. **44, 45** — *Braarudosphaera bigelowii* (Gran & Braarud, 1935) Deflandre 1947. Sample 39.20–39.22 m.

Table 1: Subdivision of the borehole Baden-Sooss based on the abundance pattern of *Coccolithus pelagicus*.

Interval	Depth in m (samples)	<i>C. pelagicus</i> %	Mean %	Median %
6	8 to 22.00–22.03	3.6 to 9.7	7.12	6.37
5	22.00–22.03 to 37.20–37.22	1.3 to 16	8.09	7.47
4	37.20–37.22 to 48.00–48.02	0.8 to 9.6	4.62	3.58
3	48.00–48.02 to 78.00–78.02	0.9 to 12.3	5.54	5.03
2	78.00–78.02 to 98.00–98.02	0 to 5.4	3.12	3.27
1	98.00–98.02 to 101.80–101.82	2.7 to 14.8	5.40	4.26

Table 2: Subdivision of the borehole Baden-Sooss based on the abundance pattern of *Reticulofenestra pseudoumbilica*.

Section	Depth in m (samples)	<i>Reticulofenestra</i> <i>pseudoumbilica</i> %	Mean %	Median %
3D	8 to 21.20	0 to 7.1	2.51	1.86
3C	21.20 to 34.00–34.02	0.3 to 2.3	1.14	0.97
3B	34.00–34.02 to 48.00–48.02	0.9 to 7.8	4.57	3.92
3A	48.00–48.02 to 55.00–55.02	0.9 to 4.8	2.48	2.48
2	55.00–55.02 to 80.00–80.02	3.9 to 19.4	9.29	8.74
1	80.00–80.02 to 101.80–101.82	0.6 to 8.8	4.87	4.61

Table 3: Subdivision of the borehole Baden-Sooss based on the abundance pattern of *Reticulofenestra minuta*.

Interval	Depth in m (samples)	<i>Reticulofenestra</i> <i>minuta</i> %	Mean %	Median %
6	8 to 15.20–15.22	48.8 to 74.2	60.69	61.01
5	15.20–15.22 to 31.20–31.23	56.7 to 85.1	72.53	73.35
4	31.20–31.23 to 42.00–42.02	42.9 to 65.2	55.58	58.02
3	42.00–42.02 to 60.00–60.02	63.1 to 89	75.32	76.44
2	60.00–60.02 to 78.00–78.02	41.4 to 70.9	55.47	53.75
1	78.00–78.02 to 101.80–101.82	46.6 to 86.5	69.98	70.49

Table 4: Subdivision of the borehole Baden-Sooss based on the abundance pattern of *Umbilicosphaera jafarii*.

Interval	Depth in m (samples)	<i>Umbilicosphaera</i> <i>jafarii</i> %	Mean %	Median %
6	8 to 36.00–36.02	0 to 13.8	4.43	4.15
5	36.00–36.02 to 43.00–43.02	6.4 to 23.6	12.79	10.48
4	43.00–43.02 to 61.00–61.02	0 to 9.9	1.67	0.78
3	61.00–61.02 to 70.00–70.02	1.9 to 29.3	15.31	16.19
2	70.00–70.02 to 88.00–88.02	1.9 to 12.5	6.97	7.39
1	88.00–88.02 to 101.80–101.82	0 to 4.9	1.71	1.04

Table 5: Subdivision of the borehole Baden-Sooss based on the abundance patterns of *S. heteromorphus* and *S. moriformis*.

Interval	Depth in m (samples)	<i>Sphenolithus</i> <i>heteromorphus</i> + <i>S. moriformis</i> %	Mean %	Median %
6	8 to 31.20–31.23	0 to 2.9	0.81	0.45
5	31.20–31.23 to 49.00–49.02	0 to 4.2	1.47	1.49
4	49.00–49.02 to 61.00–61.02	0 to 0.6	0.26	0.30
3	61.00–61.02 to 79.00–79.02	0 to 1.6	0.55	0.33
2	79.00–79.02 to 93.00–93.02	0 to 2.9	1.27	1.17
1	93.00–93.02 to 101.80–101.82	0 to 1.3	0.29	0.12

Table 6: Subdivision of the borehole Baden-Sooss based on the abundance pattern of reworked specimens.

Interval	Depth in m (samples)	Reworked %	Mean %	Median %
6	8 to 15.20–15.22	0.3 to 17.8	10.6	13.77
5	15.20–15.22 to 28.00–28.02	0 to 19.6	3.55	2.5
4	28.00–28.02 to 48.00–48.02	0 to 8.4	2.65	1.76
3	48.00–48.02 to 81.00–81.02	0 to 2.5	1.07	0.95
2	81.00–81.02 to 94.00–94.02	0 to 4.04	1.44	1.5
1	94.00–94.02 to 101.80–101.82	0 to 0.9	0.38	0.33

cated on the left side of the first axis and range in the second axis from the centre to the lower part (Fig. 5).

All species again are present in **Cluster 3**, but with other species possessing high indicator values (Table 10). *Coccolithus pelagicus* (IV 36) is accompanied by *H. carteri* (IV 33), thus both are separated from the remaining species that possess IV's less than 25. But the most significant components are 'reworked species' with a IV of 38. Samples of Cluster 3 are located in nMDS in the centre of the first axis similar to Cluster 1, but in contrast to the latter they are concentrated in the upper part of the second axis (Fig. 5).

All species can be found in **Cluster 4** (Fig. 4, Table 10), with *Umbilicosphaera jafarii* as the main indicator species (IV 43), accompanied by *R. pseudoumbilica* (IV 32). While in nMDS samples belonging to Cluster 4 are positioned in the centre of the second axis, they dominate the right part of the first axis (Fig. 5).

The sequence of clusters along the core is shown in Fig. 6b, where intensities of changes in the floral composition are also figured (Fig. 6c). The first interval (**Period 1**) from 77 to 102 m is characterized by samples alternating between Clusters 1 and 2. It can be partitioned into three sections, where in the first section (**Period 1.1**) between 94 and 102 m the samples behave constantly and are located in nMDS in the intermingling zone between Clusters 1 and 2 (Fig. 5). The following **Period 1.2** between 88 and 94 m is characterized by stronger sample oscillations between Clusters 1 and 2. The last subinterval (**Period 1.3**) between 77 and 88 m remains more or less constantly with a dominance of samples belonging to Cluster 2. After a strong change at 77 m the next interval (**Period 2**) shows samples mainly belonging to Cluster 3 (Fig. 6c). Period 2 is abruptly finished at 71 m. **Period 3** starts with strong sample alterations between Clusters 2 and 4 in the first 3 meters, afterwards remaining constant until 61 m with samples belonging to Cluster 4. The following interval between 41 and 61 m (**Period 4**) shows a differentiation into 3 sub-intervals. **Period 4.1** ranging from 54 to 61 m is distinguished by low oscillating samples belonging to Cluster 2. Strong oscillations within Cluster 2 and some contact to Cluster 3 marks samples of the interval between 48 and 54 m (**Period 4.2**). The last interval (**Period 4.3**) is characterized by a minor trend in samples from Cluster 2 to Cluster 1. The strongest oscillations in nanoplankton compositions can be found in the interval between 34 and 41 m (**Period 5**), where samples belonging to Clusters 1, 3 and 4 alternate intensively (Fig. 5c). Samples of the following **Period 6** from 23 to 34 m behave more constantly showing a slight tendency from Clusters 3 and 2 to Cluster 1. This tendency is abruptly interrupted at 22 m (the single sample belongs to Cluster 3) followed by **Period 7**, where all samples belong to Cluster 2. This period again is abruptly finished at 14 m (the single sample belongs to Cluster 4) and samples of the following **Period 8** (from 10 to 13 m) are members of Cluster 3. The last 2 samples (8 and 9 m) belong to Clusters 1 and 2.

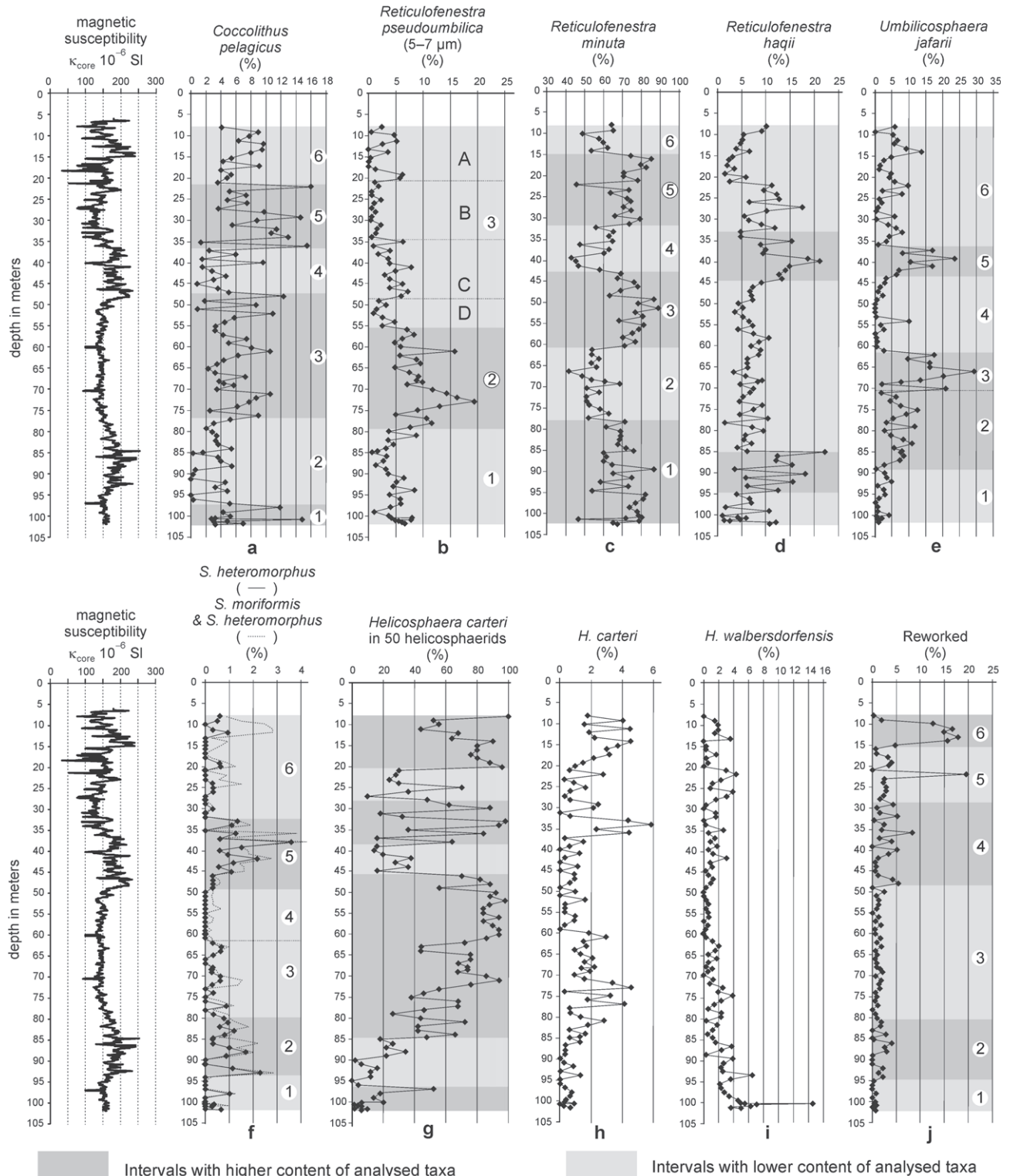


Fig. 3. a-j — Distribution patterns of selected calcareous nannofossils in the Baden-Soos core, plotted versus depth and their relation to magnetic susceptibility.

Discussion

In a first step, the environmental behaviour of the prominent species will be discussed. Among the nannoplankton, *Coccolithus pelagicus* is well known as an important paleo-

ecologic marker. This species as an r-strategist is abundant in cold water (Okada & McInyre 1979; Winter et al. 1994). A high amount of *C. pelagicus* indicates higher nutrient levels and eutrophic conditions. This species occurs at water temperatures between -1.5° and $+15^{\circ}$ C, with the highest

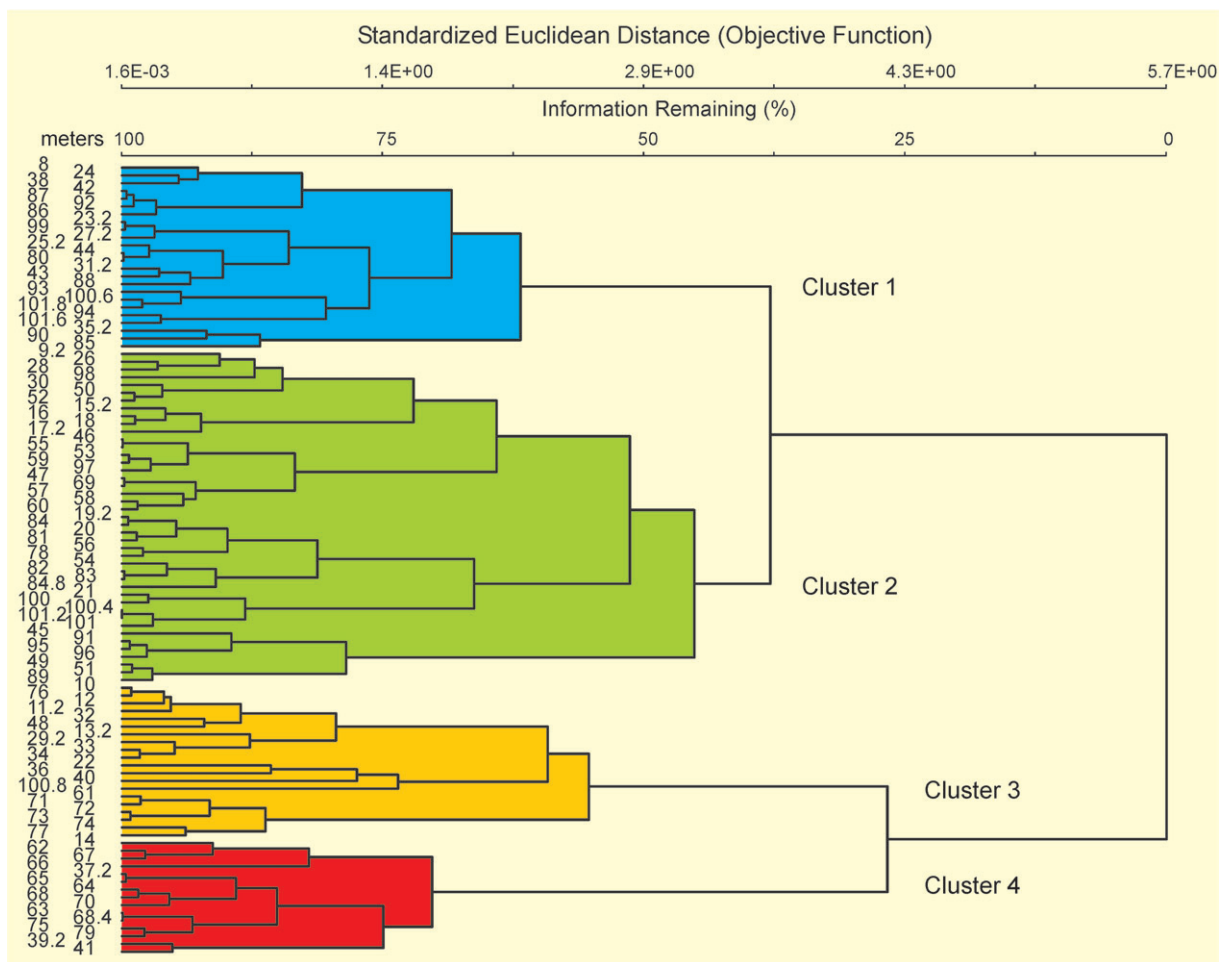


Fig. 4. Dendrogram of sample clusters resulting from Ward's method.

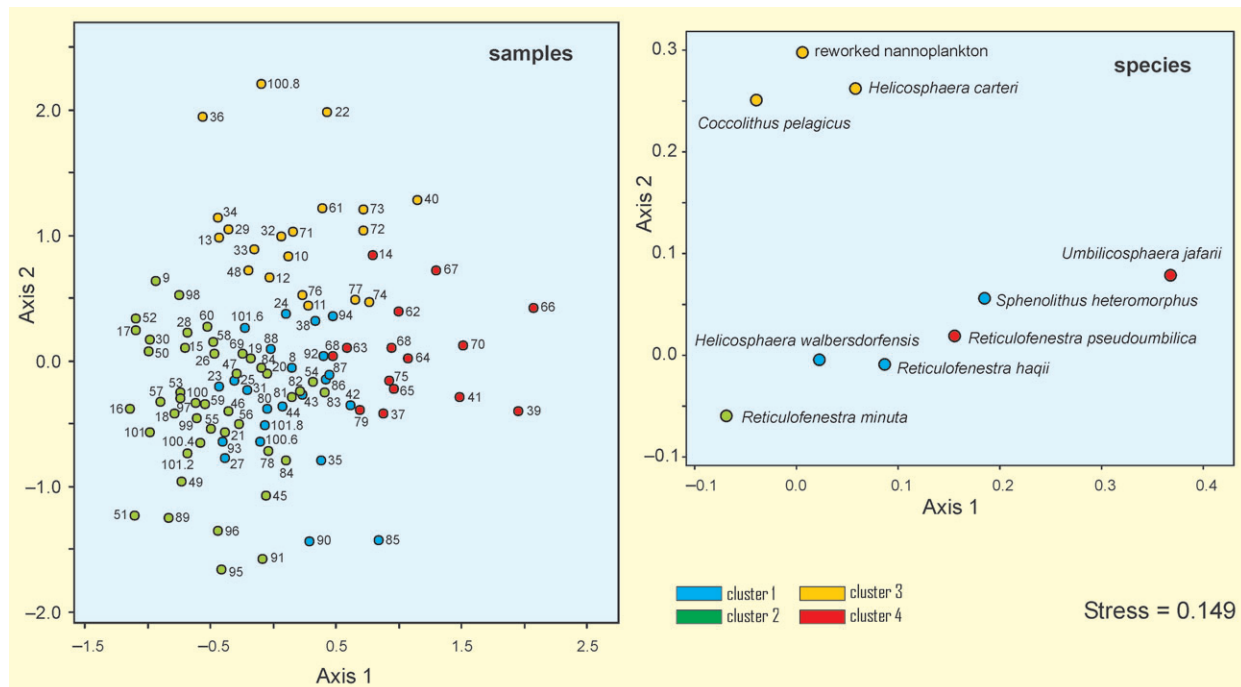


Fig. 5. Nonmetrical Multidimensional Scaling (nMDS) of samples and position of species in the axes system.

Table 7: The distribution of autochthonous calcareous nannofossils in the borehole Baden-Sooss, alphabetically arranged.

Species	Specimen number	Number of samples
<i>Acanthoica cohenii</i> (Jerkovic, 1971) Aubry, 1999	85	41
<i>Braarudosphaera bigelowii</i> (Gran & Braarud, 1935) Deflandre, 1947	57	39
<i>Calcidiscus leptoporus</i> (Murray & Blackman, 1898) Loeblich & Tappan, 1978	31	22
<i>Calcidiscus premacyntirei</i> Theodoridis, 1984	6	3
<i>Calcidiscus tropicus</i> Kamptner, 1956	2	2
<i>Calciosolenia murrayi</i> Gran, 1912	1	1
<i>Coccolithus miopelagicus</i> Bukry, 1971	25	20
<i>Coccolithus pelagicus</i> (Wallich, 1871) Schiller, 1930	1855	100
<i>Coccolithus</i> sp.	9	9
<i>Coronocyclus nitescens</i> (Kamptner, 1963) Bramlette & Wilcoxon, 1967	40	30
<i>Coronosphaera mediterranea</i> (Lohmann, 1902) Gaarder, 1977	202	78
<i>Cryptococcolithus mediaperforatus</i> (Varol, 1991) de Kaenel & Villa, 1996	82	36
<i>Cyclcargolithus floridanus</i> (Roth & Hay, 1967) Bukry, 1971	243	68
<i>Discoaster adamanteus</i> Bramlette & Wilcoxon, 1967	8	8
<i>Discoaster deflandrei</i> Bramlette & Riedel, 1954	4	4
<i>Discoaster exilis</i> Martini & Bramlette, 1963	5	5
<i>Discoaster formosus</i> Martini & Worsley, 1971	6	4
<i>Discoaster musicus</i> Stradner, 1959	11	9
<i>Discoaster sanmiguelensis</i> Bukry, 1981	3	2
<i>Discoaster variabilis</i> Martini & Bramlette, 1963	20	15
<i>Discoaster</i> sp.	8	7
<i>Geminitihella rotula</i> Kamptner, 1956	150	63
<i>Hayella challengerii</i> (Müller, 1974) Theodoridis, 1984	32	23
<i>Helicosphaera carteri</i> (Wallich, 1877) Kamptner, 1954	446	90
<i>Helicosphaera euphratis</i> Haq, 1966	6	6
<i>Helicosphaera granulata</i> (Bukry & Percival, 1971) Jafar & Martini, 1975	1	1
<i>Helicosphaera minuta</i> Müller, 1981	74	45
<i>Helicosphaera vedderi</i> Bukry, 1981	3	3
<i>Helicosphaera walbersdorffensis</i> Müller, 1974	625	93
<i>Helicosphaera wallachi</i> (Lohmann, 1902) Boudreux & Hay, 1969	3	2
<i>Helicosphaera</i> sp.	4	3
<i>Holodiscolithus macroporus</i> (Deflandre, 1954) Roth, 1970	55	39
<i>Ilselithina fusa</i> Roth, 1970	19	14
<i>Lithostromation perdurum</i> Deflandre, 1942	2	2
<i>Micrantholithus articulatus</i> Bukry & Percival, 1971	14	13
<i>Micrantholithus flos</i> Deflandre, 1954	11	9
<i>Micrantholithus vesper</i> Deflandre, 1950	50	37
<i>Perforocalcinella fusiformis</i> Bona, 1964	4	4
<i>Pontosphaera discopora</i> Schiller, 1925	2	2
<i>Pontosphaera multipora</i> (Kamptner, 1948) Roth, 1970	94	56
<i>Pyrocyclus orangensis</i> (Bukry, 1971) Backman, 1980	3	2
<i>Reticulofenestra gelida</i> (Geitzenauer, 1972) Backman, 1978	279	82
<i>Reticulofenestra hagii</i> Backman, 1978	2596	102
<i>Reticulofenestra minuta</i> Roth, 1970	22467	102
<i>Reticulofenestra pseudoumbilicus</i> (Gartner, 1967) Gartner, 1969	1685	99
<i>Reticulofenestra</i> sp.	83	33
<i>Rhabdosphaera clavigera</i> Murray & Blackman, 1898	10	9
<i>Rhabdosphaera pannonica</i> Báldi-Beke, 1960	2	2
<i>Rhabdosphaera procerata</i> Martini, 1969	2	2
<i>Rhabdosphaera sicca</i> Stradner, 1963	110	58
<i>Rhabdosphaera</i> sp.	6	6
<i>Sphenolithus abies</i> Deflandre, 1954	2	2
<i>Sphenolithus heteromorphus</i> Deflandre, 1953	140	57
<i>Sphenolithus milanetti</i> Olafsson & Rio	3	3
<i>Sphenolithus moriformis</i> (Brönnimann & Stradner, 1960) Bramlette & Wilcoxon, 1967	129	59
<i>Sphenolithus</i> sp.	13	11
<i>Syracosphaera pulchra</i> Lohmann, 1902	51	36
<i>Thoracosphaera heimii</i> (Lohmann, 1919) Kamptner, 1941	5	5
<i>Thoracosphaera saxeae</i> Stradner, 1961	7	7
<i>Triquetrorhabdulus challengerii</i> Perch-Nielsen, 1971	1	1
<i>Triquetrorhabdulus milowii</i> Bukry, 1971	4	4
<i>Triquetrorhabdulus</i> sp.	1	1
<i>Umbilicosphaera jafarii</i> Müller, 1974	1828	96

concentration found between +2° and +12 °C. Higher percentages of *C. pelagicus* were documented in the Lower Miocene (Karpatian, Laa Fm) and the lowermost part of the Middle Miocene (clastic sequence of the Lower Badenian) from the borehole Roggendorf-1 in the neighbouring Molasse Basin (Ćorić & Rögl 2004). Higher percentages of *C. pelagicus* in nannoplankton assemblages during intervals 1, 3 and 5 indicate cooling, whereas lower values in intervals 2, 4 and 6 point to slight warming during these periods.

Haq (1980) concluded that small **reticulofenestrids** dominate nannoplankton assemblages along continental margins. They were used for the paleoecological interpretation of Lower/Middle Miocene sediments from the borehole Roggendorf-1 in the Austrian Alpine-Carpathian Foredeep (Molasse Basin; Ćorić & Rögl 2004). Blooms of *Reticulofenestra minuta* in Badenian sediments were interpreted as indicators of a warmer, better-stratified water column in contrast to Karpatian assemblages with dominance of *C. pelagicus*. High numbers of small reticulofenestrids (*Reticulofenestra minuta*) were also documented by Tomanová Petrová & Švábenická (2006) in the Carpathian Foredeep, Moravia in the Lower Badenian strata. Wade & Bown (2006) investigated the co-occurrence of diatoms and abundant *Reticulofenestra minuta* in extreme paleoenvironments during the Messinian salinity crises in the Polemi Basin (Cyprus). They concluded that this species tolerates brackish to hypersaline environments. Abundant *R. minuta* in low diversity assemblages occurs there before and after the deposition of evaporates (Wade & Bown 2006).

Umbilicosphaera jafarii is widespread in Badenian sediments from the Central Paratethys. The paleo-ecology of this form is not well known yet. Wade & Bown (2006) found that *U. jafarii* flourishes in shallow water and the dominance in nannoplankton assemblages points to hypersaline paleoconditions. Higher percentages of *U. jafarii* in the intervals 3 and 5 could point to slightly increased salinity.

Table 8: a — The distribution of calcareous nannofossils reworked from the Paleogene/Early Neogene in the borehole Baden-Sooss, alphabetically arranged. **b** — The distribution of calcareous nannofossils reworked from the Cretaceous in the borehole Baden-Sooss, alphabetically arranged.

a

Species	Specimen number	Number of samples
<i>Biantholithus</i> sp.	1	1
<i>Blackites</i> sp.	2	1
<i>Chiasmolithus grandis</i> (Bramlette & Riedel, 1964) Radomski, 1968	3	2
<i>Chiasmolithus</i> sp.	3	3
<i>Clausiococcus fenestratus</i> (Deflandre & Fert, 1954) Prins, 1979	2	2
<i>Cribrocentrum reticulatum</i> (Gartner & Smith, 1967) Perch-Nielsen, 1971	1	1
<i>Cruciplacolithus</i> sp.	1	1
<i>Discoaster barbadiensis</i> Tan, 1927	2	2
<i>Discoaster gemmeus</i> Stradner, 1959	3	3
<i>Discoaster kuepperi</i> Stradner, 1959	17	12
<i>Discoaster lodoensis</i> Bramlette & Riedel, 1954	22	18
<i>Discoaster mirus</i> Deflandre, 1954	3	3
<i>Discoaster multiradiatus</i> Bramlette & Riedel, 1954	19	16
<i>Discoaster tanii</i> Bramlette & Riedel, 1954	1	1
<i>Discoaster</i> sp.	19	11
<i>Ellipsolithus macellus</i> (Bramlette & Sullivan, 1961) Sullivan, 1964	2	2
<i>Ericsonia formosa</i> (Kamptner, 1954) Haq, 1971	20	17
<i>Ericsonia robusta</i> (Bramlette & Sullivan, 1961) Edwards & Perch-Nielsen, 1975	2	2
<i>Fascicullithus</i> sp.	1	1
<i>Helicosphaera lophota</i> Bramlette & Sullivan, 1961	3	3
<i>Helicosphaera mediterranea</i> Müller, 1981	1	1
<i>Neochiastozygus</i> sp.	3	3
<i>Pontosphaera duocava</i> (Bramlette & Sullivan, 1961) Romein, 1979	1	1
<i>Prinsius martinii</i> (Perch-Nielsen, 1969) Haq, 1971	14	13
<i>Reticulofenestra bisecta</i> (Hay, 1966) Roth, 1970	6	6
<i>Reticulofenestra dictyoda</i> (Deflandre, 1954) Stradner, 1968	11	6
<i>Sphenolithus conicus</i> Bukry, 1971	1	1
<i>Sphenolithus disblemanni</i> Fornaciari & Rio, 1996	2	2
<i>Sphenolithus editus</i> Perch-Nielsen, 1978	1	1
<i>Sphenolithus furcatolithoides</i> Locker, 1967	1	1
<i>Sphenolithus radians</i> Deflandre, 1952	23	18
<i>Sphenolithus spiniger</i> Bukry, 1971	2	2
<i>Toweius</i> sp.	234	53
<i>Tibrachiatius orthostylus</i> Shamarai, 1963	11	10
<i>Zygrhablithus bijugatus</i> (Deflandre, 1954) Deflandre, 1959	44	26

b

Species	Specimen number	Number of samples
<i>Arkhangelskiella cymbiformis</i> Vekshina, 1959	12	9
<i>Arkhangelskiella maastrichtiana</i> Burnett, 1998	2	2
<i>Biscutum ellipticum</i> (Górka, 1957) Grün, 1975	9	5
<i>Broinsonia parca</i> (Stradner, 1963) Bukry, 1969 ssp. <i>constricta</i> Hattner et al. 1980	4	4
<i>Calculosites obscurus</i> (Deflandre, 1959) Prins & Sissingh, 1977	6	5
<i>Ceratolithoides sesquipedalis</i> Burnett, 1998	2	1
<i>Cribrosphaerella ehrenbergii</i> (Arkhangelsky, 1912) Deflandre, 1952	6	3
<i>Cyclagelosphaera reinhardtii</i> (Perch-Nielsen, 1968) Romein, 1977	5	5
<i>Eiffellithus gorkae</i> Reinhardt, 1965	13	12
<i>Eiffellithus turriseiffeltii</i> (Deflandre, 1954) Reinhardt, 1965	3	3
<i>Lucianorhabdus cayexii</i> Deflandre, 1959	1	1
<i>Microrhabdulus decoratus</i> Deflandre, 1959	3	3
<i>Micula decussata</i> Vekshina, 1959	47	21
<i>Placozygus fibuliformis</i> (Reinhardt, 1964) Hoffmann, 1970	8	8
<i>Prediscosphaera cretacea</i> (Arkhangelsky, 1912) Gartner, 1968	33	16
<i>Reinhardtites levii</i> Prins & Sissingh, 1977	4	3
<i>Retecapsa crenulata</i> (Bramlette & Martini, 1964) Grün, 1975	4	4
<i>Uniplanarius gothicus</i> (Deflandre, 1959) Hattner & Wise, 1980	2	2
<i>Watznaueria barnesae</i> (Black, 1959) Perch-Nielsen, 1968	192	70
<i>Watznaueria biporta</i> Bukry, 1969	2	2
<i>Watznaueria britannica</i> (Stradner, 1963) Reinhardt, 1964	7	7
<i>Watznaueria fossacincta</i> (Black, 1971) Bown, 1989	12	10
<i>Zeugrhabdotus diplogrammus</i> (Deflandre, 1954) Burnett, 1996	4	4

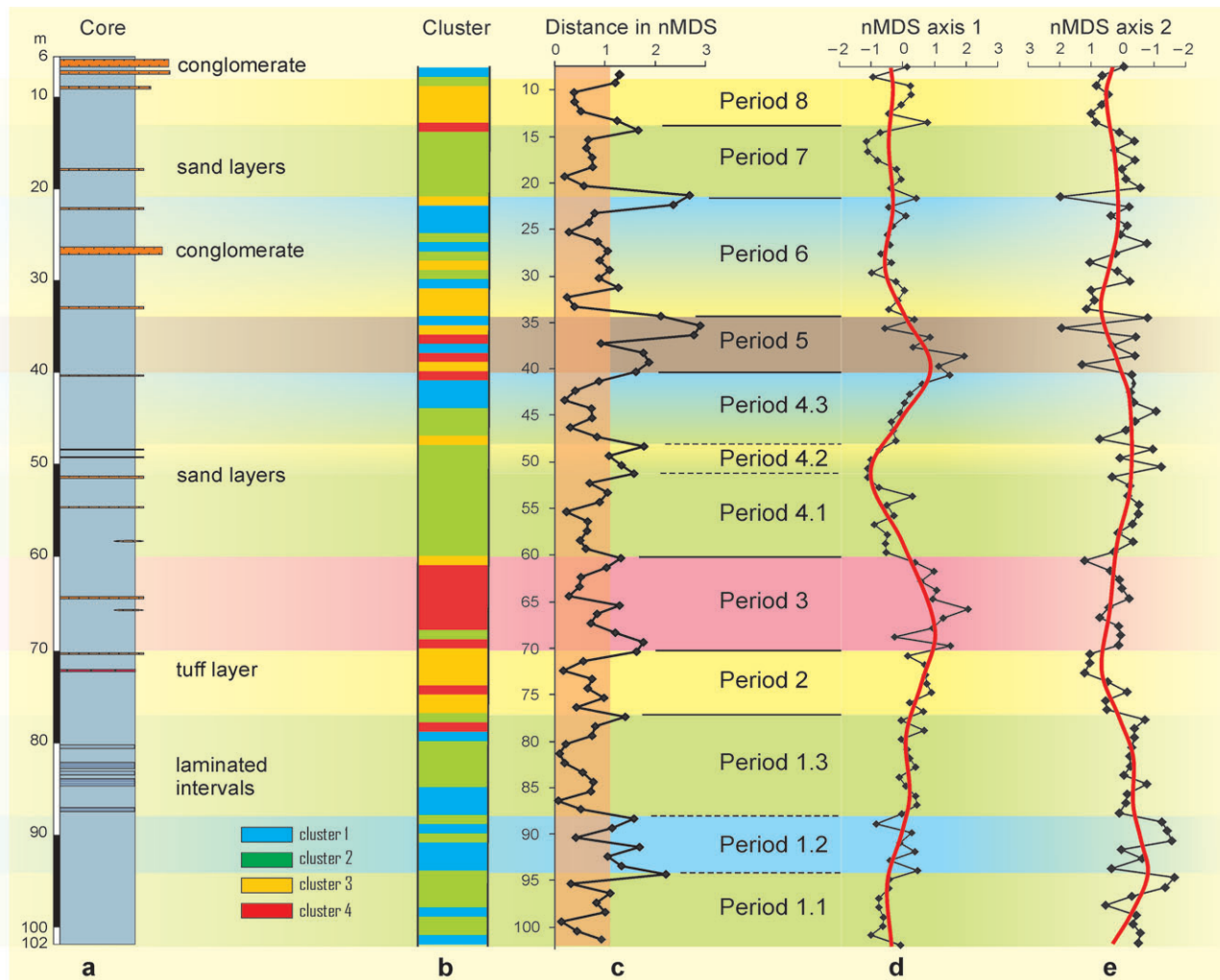


Fig. 6. **a** — Sedimentary characteristic of the core. **b** — Cluster sequence along the core. **c** — Dissimilarities in community composition between subsequent samples. **d** — Sequence of sample values in axis 1 of nMDS and fit by sinusoidal regression. **e** — Sequence of sample values in axis 2 of nMDS and fit by sinusoidal regression.

The main and extremely significant negative correlation of *U. jafarii* with *R. minuta* confirms the response of *U. jafarii* to elevated salinity conditions in contrast to *R. minuta*, which seems to be characteristic for slightly lowered salinities.

Perch-Nielsen (1985) concluded that **sphenoliths** occurred in shallow environments. Generally they preferred warm waters. They were common in oligotrophic environments.

Helicoliths are common in shallow, near continental environments indicating an upwelling regime (Perch-Nielsen 1985). A slight enrichment of ***Helicosphaera carteri*** in three intervals points to turbulent water during these periods. This is also indicated by the high correlation with *C. pelagicus* and the ‘reworked nannoplankton’ together with the strong negative correlation to *R. minuta*, because the latter indicates quieter conditions (Table 9).

Discoasterids are directly related to water temperature. This K-selected group is generally common in oligotrophic, warm and deep oceanic water. Discoasterids characterize stable paleoenvironments (Lohmann & Carlson 1981; Aubry 1992; Young 1998). Thus the highest diversifications of discoast-

erids within thanatocoenoses usually correspond to a warmer climate. Low percentages of these forms without abundance oscillations point to a sedimentation milieu close to the coast.

According to these environmental demands of the nannoplankton dominating in the core, the obtained clusters can now be interpreted as follows:

Cluster 1: This cluster seems to characterize intermediate, ‘normal’ conditions of the environment in the Baden-Soöss core, because all species can be found in this class, but with different proportions. Beside *R. minuta* that is abundant in the whole core, *R. haqii* and *H. walbersdorfensis* characterize this cluster due to higher percentages. The rare *S. heteromorphus* gets the highest indicator values within all classes (Table 10). This cluster gradually merges with Cluster 2 as demonstrated by nMDS (Fig. 5).

Cluster 2: The dominance of *R. minuta* and the virtually complete disappearance of *S. heteromorphus* hints at a paleoenvironment slightly deviating from conditions found in Cluster 1. According to the environmental demands of *R. minuta* and the lowered percentages of the other species, this

Table 9: Correlation matrix between physical-chemical parameters and nanoplankton groups. Below the correlation coefficients the probability of non-correlation is marked. Significant correlations in bold numbers.

	$\delta^{13}\text{C}$	$\delta^{18}\text{O}$	magnetic susceptibility	<i>Coccolithus pelagicus</i>	<i>Reticulofenestra minuta</i>	<i>Pseudounihamella reticulofenestrata</i>	<i>Umbilicosphaera lajearii</i>	<i>Sphenolithus heteromorphus</i>	<i>Reticulofenestra haqii</i>	<i>Reticulofenestra haqii</i>	<i>Umbilicosphaera carteri</i>	<i>Helicosphaera walpersdorffensis</i>	<i>Helicosphaera carteri</i>	<i>Umbilicosphaera carteri</i>	<i>Helicosphaera walpersdorffensis</i>	<i>Umbilicosphaera lajearii</i>	<i>Sphenolithus heteromorphus</i>	<i>Reticulofenestra minuta</i>	<i>Pseudounihamella reticulofenestrata</i>	<i>Umbilicosphaera lajearii</i>	<i>Helicosphaera carteri</i>	<i>Umbilicosphaera carteri</i>	<i>Helicosphaera walpersdorffensis</i>	reworked	
<i>Coccolithus pelagicus</i>	-0.226 0.057	0.162 0.173	0.207 0.081	1	-0.180 0.130	-0.264 0.025	-0.148 0.214	-0.094 0.433	0.034 0.779	0.466 0.000	-0.179 0.133	0.502 0.000													
<i>Reticulofenestra pseudounihamella</i>	0.021	-0.095	-0.001	-0.180 0.130	1	-0.331 0.004	-0.003 0.980	0.193 0.104	-0.028 0.817	-0.052 0.663	-0.039 0.745	-0.172 0.149													
<i>Reticulofenestra minuta</i>	0.836	0.428	0.993	-0.115 0.337	-0.264 0.025	-0.331 0.004	1	-0.471 0.000	-0.715 0.000	-0.257 0.030	-0.046 0.002	-0.359 0.002													
<i>Reticulofenestra haqii</i>	0.193	-0.046	0.115	-0.062 0.249	-0.138 0.249	-0.148 0.224	-0.003 0.980	-0.471 0.000	1	0.186 0.118	0.259 0.028	-0.174 0.145	0.024 0.784	0.033 0.844	0.024 0.844	0.024 0.844	0.024 0.844	0.024 0.844	0.024 0.844	0.024 0.844	0.024 0.844	0.024 0.844	0.024 0.844		
<i>Umbilicosphaera jafarii</i>	0.220 0.064	0.094 0.431	-0.157 0.188	-0.094 0.433	0.193 0.104	-0.715 0.000	0.186 0.118	1	0.195 0.101	0.210 0.076	0.030 0.802	0.084 0.481													
<i>Sphenolithus heteromorphus</i>	0.415 0.000	-0.076 0.525	-0.188 0.114	-0.034 0.779	-0.028 0.817	-0.257 0.030	0.259 0.028	0.195 0.101	1	-0.013 0.913	-0.049 0.685	0.112 0.349													
<i>Helicosphaera carteri</i>	-0.010	0.018	-0.101	0.466 0.000	-0.052 0.663	-0.358 0.002	-0.174 0.145	0.210 0.076	-0.013 0.913	1	-0.253 0.032	0.452 0.000													
<i>Helicosphaera walpersdorffensis</i>	0.933	0.879	0.397	0.000	0.663	0.502 0.133	-0.039 0.745	-0.046 0.701	0.033 0.784	0.030 0.802	-0.049 0.685	-0.253 0.032	1	-0.102 0.396											
reworked	0.0229	0.160	-0.094	0.502 0.000	-0.172 0.149	-0.359 0.024	0.024 0.844	0.084 0.844	0.112 0.481	0.112 0.349	0.452 0.000	-0.102 0.396													
	0.053	0.180	0.434	0.053	0.149	0.000																			

cluster may indicate a marginally lowered salinity and slightly elevated temperatures.

Cluster 3: Lowered temperatures and higher nutrient levels characterizing a shift to eutrophic conditions are indicated by high proportions of *C. pelagicus* (Table 10). Therefore, this cluster may indicate non-stratified turbulent water masses.

Cluster 4: The main species in this cluster is *U. jafarii* demonstrating the highest indicator values within all species (Table 10). The opposite role of *U. jafarii* to *R. minuta* is first demonstrated by the highest negative correlation within all comparisons between species (Table 9) and second by the opposite positions within nMDS axis 1 (Fig. 5). This confirms the interpretation of Wade & Bown (2006) that *U. jafarii* preferred hypersaline conditions, and so Cluster 4 may indicate slightly elevated salinity caused by well-stratified water masses.

According to the environmental interpretations of Cluster 1 to 4, their position within the nMDS axis allows an interpretation of axes as environmental gradients (Fig. 5). The position of the characteristic species *R. minuta* at lower values of Axis 2 and *C. pelagicus* at the higher values allows an equalization of Axis 2 with a decreasing temperature gradient, where the range of this gradient does not seem to be enormous. Similar to this interpretation, the positions of *R. minuta* and *U. jafarii* on opposite sides of Axis 1 (Fig. 5) allows its equalization with an increasing salinity gradient. Again, the range in salinity should be within euhaline conditions.

Values of the nMDS-axes can now be used for determining trends in salinity and paleotemperature along the core (Fig. 5d and 5e), which also explains the changes in different periods:

During **Period 1** (77 to 102 m) a salinity increase is coupled with rising temperatures that peak in Subperiod 1.2. While during Subperiod 1.3 salinity continues to increase, temperature slightly decreases. Salinity still increases during **Period 2** (71 to 77 m), but temperature declines to a local minimum in the temperature curve (Fig. 6) that is reached at the boundary to the following interval. This minimum is expressed in the higher proportion of *C. pelagicus*. The salinity maximum can be found in **Period 3** (61 to 71 m), while temperature starts to increase at the beginning of this period (Fig. 6). The dominance of Cluster 4 with *U. jafarii* is characteristic. Salinity is low during **Period 4** (41 to 61 m), where it reaches the absolute minimum in the middle of this period (Subperiod 4.2), starting to increase in the last Subperiod 4.3 (Fig. 6). Temperature demon-

Table 10: Indicator values of species for clusters obtained by Ward's method based on standardized Euclidean Distances. Highest indicator values in bold numbers.

	Cluster 1	Cluster 2	Cluster 3	Cluster 4
	24 samples	43 samples	20 samples	15 samples
<i>Coccolithus pelagicus</i>	21	21	36	21
<i>Reticulofenestra pseudoumbilica</i>	20	21	25	32
<i>Reticulofenestra minuta</i>	26	29	23	22
<i>Reticulofenestra haqii</i>	32	19	24	25
<i>Umbilicosphaera jafarii</i>	19	12	24	43
<i>Sphenolithus heteromorphus</i>	22	7	14	20
<i>Helicosphaera carteri</i>	15	17	33	28
<i>Helicosphaera walbersdorffensis</i>	30	18	25	19
reworked	20	19	38	22

strates the opposite trend by reaching a local maximum during Subperiod 4.2. **Period 5** (34 to 41 m) resembles Period 3 in having a salinity maximum at the beginning of the period, but temperature behaves opposite to Period 3 in this period by becoming colder. The strong oscillations between clusters within this period (Fig. 6c) could be affected by the loss of sedimentation (and time) in the upper core part due to high tectonic activity (Hohenegger et al. 2008). Salinity decreases at the beginning of **Period 6** (23 to 34 m) and remains constant during Periods 7 and 8 until the end of the core. This trend positively deviates at 14, making a clear boundary between Periods 7 and 8. This extreme deviation at a single sample could also be based on tectonics affecting a loss in sedimentation. This assumption is supported by high dissimilarities in community composition both to the preceding and subsequent sample (Fig. 6c). The temperature increases constantly during Period 6, but is interrupted by a significant falling off at 22 m, again caused by sedimentation loss, marking the border to the following period. Salinity shows a local minimum during **Period 7** (15 to 21 m), while temperature decreases slightly (Fig. 6). Salinity remains constant at a medium level during **Period 8** (10 to 13 m), but temperature shows a local minimum returning to 'normal' conditions in the two uppermost core meters.

Conclusions

All investigated samples from the scientific borehole Baden-Sooss contain common and well-preserved nannoplankton assemblages dominated by the genera *Reticulofenestra*, *Coccolithus* and *Umbilicosphaera*.

Biostratigraphically, the borehole Baden-Sooss can be assigned to nannoplankton Zone NN5 (*S. heteromorphus* Zone of Martini 1971), indicating an Early Badenian age. The low concentration of *H. walbersdorffensis* allows correlation with the MNN5a (*S. heteromorphus*-*H. walbersdorffensis* Interval Subzone of Fornaciari et al. 1996).

The following calcareous nannoplankton species were analysed for paleoecological interpretation: *C. pelagicus*, discoasterids, helicosphaerids, reticulofenestrids (*R. minuta*, *R. pseudoumbilicus*), sphenoliths (*S. heteromorphus*, *S. moriformis*), *U. jafarii*, and the participation of reworked nannoplankton from older strata. *Coccolithus pelagicus* is negatively correlated with magnetic susceptibility, thus

higher percentages of this form coincide with lower values of magnetic susceptibility and suggest lower water temperature. On the other hand, lower percentages of *C. pelagicus* can be correlated with peaks of magnetic susceptibility. These periods suggest warmer water due to the higher insolation. Periods of colder, non-stratified water containing higher proportions of *C. pelagicus* are concentrated in the deeper core between 71 and 77 m, when it was replaced in the following period by stratified, higher salinity and warmer water. A slight, but continual temperature decrease starting from 50 m core-depth upwards results in an abundance increase of *C. pelagicus* also signalizing an eutrophication trend.

Small reticulofenestrids, which occupy marine environments along continental margins, dominate the nannoplankton assemblages in the core. Oscillations in abundances of these species could signalize changes in temperature inferring warmer, stratified water and lower salinity.

Sphenoliths can also be used as temperature indicators. Therefore, higher percentages of *S. heteromorphus* and *S. moriformis* coincide with increased magnetic susceptibility.

Umbilicosphaera jafarii is common in shallow environments; and the abundance peaks reflect a slight increase in salinity. The transition from a community with abundant *C. pelagicus* to *U. jafarii* needs a slight temperature increase, thus these transitions are often found in the core. Transitions from communities with abundant *U. jafarii* to communities, where *R. minuta* dominates, are discontinuous needing larger and abrupt environmental changes.

The higher erosion rate on the continent is documented by high percentages of reworked calcareous nannoplankton. This can be correlated with the intensified input of magnetic particles as documented by magnetic susceptibility.

Low percentages of discoasterids point to a sedimentation milieu close to the shoreline.

The low variation in nannofossil assemblages of the Baden-Sooss core suggests relatively low fluctuating environments during this part of the Lower Badenian. Changes in the structure of nannoplankton assemblages occurred in periods that could be related to fluctuations in the Milankovich astronomical cycles. In the upper core (8 to 40 m) diminution of the sediment record due to tectonics is pictured, on the one side, in higher cluster oscillations between 34 and 40 m and, on the other, in the abrupt intercalation of samples (at 22 m and 14 m) distinctly deviating from samples that are homogeneous or continually changing within periods.

Acknowledgments: This study was financially supported by the Austrian Science Foundation FWF Project P16793-B06. Thanks are due to the whole group working in the above project, especially to Christian Rupp (Geological Survey, Wien), Peter Pervesler, Karl Stingl (Institute of Palaeontology, Universität Wien), Fred Rögl (Natural History Museum, Wien), Anna Selge, Robert Scholger (Institute of Geophysics, Montan Universität Leoben), Maksuda Khatun, Michael Wagreich (Department of Geodynamics and Sedimentology, Universität Wien) and Nils Andersen (Leibniz Laboratory, CAUniversity Kiel).

References

- Aubry M.P. 1992: Late Paleogene calcareous nannoplankton evolution: a tale of climatic deterioration. In: Prothero D.R. & Berggren W.A. (Eds.): Eocene-Oligocene climatic and biotic evolution. *Princeton University Press*, 272–309.
- Bown P.R. & Young J.R. 1998: Introduction. In: Bown P.R. (Ed.): Calcareous nannofossil biostratigraphy. *Kluwer Academic Publications*, Dordrecht, 1–15.
- Ćorić S. & Rögl F. 2004: Roggendorf-1 borehole, a key section for Lower Badenian transgressions and the stratigraphic position of the Grund Formation. *Geol. Carpathica* 55, 2, 165–178.
- Dufrène M. & Legendre P. 1997: Species assemblages and indicator species: The need for a flexible asymmetrical approach. *Ecological Monographs* 67, 3, 345–366.
- Fornaciari E. & Rio D. 1996: Latest Oligocene to early middle Miocene quantitative calcareous nannofossil biostratigraphy in the Mediterranean region. *Micropaleontology* 42, 1, 1–37.
- Fornaciari E., Di Stefano A., Rio D. & Negri A. 1996: Middle Miocene calcareous nannofossil biostratigraphy in the Mediterranean region. *Micropaleontology* 42, 1, 37–63.
- Fornaciari E., Rio D., Ghibaudo G., Massari F. & Iaccarino S. 1997: Calcareous plankton biostratigraphy of the Serravallian (Middle Miocene) stratotype section (Piedmont Tertiary Basin, NW Italy). *Mem. Sci. Geol.* 49, 127–144.
- Fuchs R. & Stradner H. 1977: Über Nannofossilien im Badenien (Mittelmiozän) der Zentralen Paratethys. *Beitr. Paläont. Österreich*, 2, 1–58.
- Gümbel C.W. 1870: Über Nulliporenkalk und Coccoolithen. *Verh. K. König. Geol. Reichsanst. Wien*, 201–203.
- Haq B.U. 1980: Biogeographic history of Miocene calcareous nannoplankton and paleoceanography of the Atlantic Ocean. *Micropaleontology* 26, 414–443.
- Hohenegger J., Ćorić S., Khatun M., Pervesler P., Rögl F., Rupp C., Selge A., Uchman A. & Wagreich M. 2008: Cyclostratigraphic dating in the Lower Badenian (Middle Miocene) of the Vienna Basin (Austria) — the Baden-Sooss core. *Int. J. Earth Sci.* DOI 10.1007/s00531-007-0287-7.
- Kamptner E. 1948: Coccoolithen aus dem Torton des Inneralpinen Wiener Beckens. *Sitz.-Ber. Österr. Akad. Wiss., Math.-Naturwiss. Kl., Abt. 1*, 157, 1–16.
- Linder A. & Berchtold W. 1976: Statistische Auswertung von Prozentzahlen. *UTB Birkhäuser Verlag*, Basel and Stuttgart, 1–232.
- Lohmann G.P. & Carlson J.J. 1981: Oceanographic significance of Pacific late Miocene calcareous nannoplankton. *Mar. Micropaleontology* 6, 553–579.
- Martini E. 1971: Standard Tertiary and Quaternary calcareous nannoplankton zonation. In: Farinacci A. (Ed.): Proceedings of the Second Planktonic Conference, Roma 1970. *Edizioni Tecno-scienza*, Roma, 739–785.
- McCune B. & Mefford M.J. 1999: PC-ORD. Multivariate analysis of ecological data, version 4. *MjM Software Design*, Gleneden Beach, Oregon, USA, 1–237.
- Okada H. & McInyre A. 1979: Seasonal distribution of the modern Coccolithophores in the western North Atlantic Ocean. *Mar. Biology* 54, 319–328.
- Perch-Nielsen K. 1985: Cenozoic calcareous nannofossils. In: Bolli H.M., Saunders J.B. & Perch-Nielsen K. (Eds.): Plankton stratigraphy. *Cambridge University Press*, 427–554.
- Rögl F., Ćorić S., Harzhauser M., Kroh A., Schultz O., Wessely G. & Zorn I. 2008: The Badenian stratotype at Baden-Sooss, Lower Austria. *Geol. Carpathica* 59, 5, 367–374.
- Sprovieri R., Bonomo S., Caruso A., di Stefano A., di Stefano E., Foresi L.M., Iaccarino S.M., Lirer F., Mazzei R. & Salvatorini G. 2002: An integrated calcareous plankton biostratigraphic scheme and biochronology for the Mediterranean Middle Miocene. *Riv. Ital. Paleont. Stratigr.* 108, 2, 337–353.
- SPSS 15.0 for Windows, 2006: Release 15.0.0. SPSS Inc.
- Stradner H. & Fuchs R. 1978: Das Nannoplankton in Österreich. In: Papp A., Cicha I., Seneš J. & Steininger F. (Eds.): Chronostratigraphie und Neostratotypen: Miozän der Zentralen Paratethys. Bd. VI. M₄, Badenien (Moravien, Wieliczen, Kosovien). *VEDA SAV*, Bratislava, 489–532.
- Švábenická L. 2002: Calcareous nannofossils of the Upper Karpatian and Lower Badenian deposits in the Carpathian Foredeep, Moravia (Czech Republic). *Geol. Carpathica* 53, 3, 197–210.
- Tomanová Petrová P. & Švábenická L. 2006: Lower Badenian biostratigraphy and paleoecology: a case study from the Carpathian Foredeep (Czech Republic). *Geol. Carpathica* 58, 4, 333–352.
- Wade B.S. & Bown P.R. 2006: Calcareous nannofossils in extreme environments: The Messinian Salinity Crisis. Polemi Basin, Cyprus. *Palaeogeogr. Palaeoclimatol. Palaeoecol.* 233, 271–286.
- Wessely G., Ćorić S., Rögl F., Draxler I. & Zorn I. 2007: Geologie und Paläontologie von Bad Vöslau (Niederösterreich). *Jb. Geol. Bundesanst.* 147, 1–2, 419–448.
- Winter A., Jordan R. & Roth P. 1994: Biogeography of living Coccolithophores in ocean waters. In: Winter A. & Siesser W. (Eds.): Coccolithophores. *Cambridge University Press*, Cambridge, 13–37.
- Young J.R. 1998: Neogene nannofossils. In: Bown P.R. (Ed.): Calcareous Nannofossil Biostratigraphy. *Kluwer Academic Publications*, Dordrecht, 225–265.

Table 1: Autochthonous calcareous nannoplankton from the Baden-Sooss core. Part 1 from 6.

Depth (m)	<i>Acanthoica cohenii</i>	<i>Braunodysphaera bigelowii</i>	<i>Calcidiscus leptopus</i>	<i>Calcidiscus premacintyrei</i>	<i>Calcidiscus tropicus</i>	<i>Calicosolenia murrayi</i>	<i>Coccilithus miopelagicus</i>	<i>Coccilithus pelagicus</i>	<i>Coccilithus sp.</i>	<i>Coronocyclus nitescens</i>	<i>Coronosphaera mediterranea</i>	<i>Cryptococcilithus medioperforatus</i>	<i>Cyclicargolithus floridanus</i>	<i>Discoaster adamanteus</i>	<i>Discoaster deflandrei</i>	<i>Discoaster exilis</i>	<i>Discoaster formosus</i>	<i>Discoaster musicus</i>	<i>Discoaster saimigneensis</i>	<i>Discoaster variabilis</i>	<i>Discoaster sp.</i>	<i>Geminithella rotula</i>		
8	1							14		7		12								x		3		
9.18–9.20	2	x	1				1	18		x		4			1					1		3		
10.0–10.03	2	x		2			3	25		1	x	14	1	1						2	2	8		
11.2–11.22	1	4	2			x	20	x		1		11										2		
12.0–12.02	1	x	x	2				31		1		17										5		
13.25–13.27	1	1					1	30		2		9										1		
14.0–14.02		1	x				2	25	x	3		8										4		
15.2–15.22			1					16		1		14	x									x		
16.0–16.02		x						13		x		1		1								x		
17.2–17.23	2	x				x	32		x	x		1										x		
18.0–18.02	4	1	2			x	13			1		x										x		
19.2–19.23	5	3				1	18		x	x	1	3										1		
20.0–20.04	x					x	15	x			2		x						1		x			
21.2	1			1		x	12		1	x		4										x		
22.0–22.03		x						52			2		3									5		
23.2–23.22	3							18		1	1		1							x		3		
24.0–24.04	x	x	x			x	25		x	1		4										3		
25.2–25.22	x	x	x	x		x	15		3	3	1	2		x										
26.0–26.02	2	1		x			23		2		x			x					1		1			
27.18–27.22	3	x					12		x	1		1												
28.0–28.02	x						30		1	x		1										x		
29.2–29.23	1	1					1	48	x	x		3		x					x		x			
30.0–30.02								29	x	x		x		x					1		x			
31.2–31.23	1	1						17			3	x		x								1		
32.0–32.02	3	7				x	35	x	4	2	x	1		1						x	1			
33.2–33.22	x					x	32	1		2	2	2									x			
34.0–34.02	3	x	1				47	x	2	6	2										1			
35.2–35.22	3	1				x	4			x	1	1									x			
36.0–36.02	2	4	1			x	49	1	1	17	8	3	x	1								1		
37.2–37.22								8														1		
38.0–38.02	x					x	20		1	8		2								x		3		
39.2–39.22	3	1				x	5	x	1		x											1		
40.0–40.02						x	32		3	5	x	1	1		2	x				x	1			
41.0–41.02	1	1				x	5	x	2	1	3					1	1	1	1	3				
42.0–42.02	x					x	9	1	2		3		x					x			2			
43.0–43.02						x	16	x	x		1					2	2	x		x				
44.0–44.02	2	x					11	x			1	1			x	x			x		x			
45.0–45.02	1	x					3	x	1		x					x			1		1			
46.0–46.02	x					x	12	1	x	1	1	x			2					2				
47.0–47.02	1					x	16		2			3	x	x		1	x				2			
48.0–48.02	1					x	39	x	1		4	1	x		1	x				1		2		
49.0–49.02	x	2				x	6		x	x	1	x		x		x	x		x	x	x			
50.0–50.02	1	x				x	27		2			2					x	x	1	x				
51.0–51.02	1	x				x	3	1	1			1				x					x			
52.0–52.02	1	1				x	34		2	2		3		x						1				
53.0–53.02	1					x	18	x	2	2		x				x					x			
54.0–54.02	x					x	14	x	1	1	2	1							x		1			
55.0–55.02						x	12	x	3	2	x				x	x			x	x	1			
56.0–56.02	2	x				x	10	x	1		x	x									1			
57.0–57.02	x					x	14	1	1	2		x	x	x		1		x	x	x				
58.0–58.02	1					x	25	x	2	1	1				1			x	2	1		x		
59.0–59.02	2	1				x	19		1		x						x		1		2			
60.0–60.02	2	x				x	26		1	2								1		3		x		

Table 1: *Continued.* Part 2 from 6.

Table 1: Continued. Part 3 from 6.

Depth (m)	<i>Hayella challengeri</i>	<i>Helicosphaera carteri</i>	<i>Helicosphaera euphratis</i>	<i>Helicosphaera granulata</i>	<i>Helicosphaera minuta</i>	<i>Helicosphaera vederi</i>	<i>Helicosphaera walbersdorffensis</i>	<i>Helicosphaera wallichii</i>	<i>Helicosphaera sp.</i>	<i>Holodiscolithus macroporus</i>	<i>Iselithina fusa</i>	<i>Lithostromatium perdurum</i>	<i>Micrantholithus articulatus</i>	<i>Micrantholithus flos</i>	<i>Micrantholithus vesper</i>	<i>Perforocalcinella fusiformis</i>	<i>Pontosphaera discopora</i>	<i>Pontosphaera japonica</i>	<i>Pontosphaera multipora</i>	<i>Pyrocyclus orangensis</i>
8	1	6(50)					x			1				x					2	
9.18–9.20	x	8(26)					3(24)			x				x						
10.0–10.03	1	5(28)	0(1)				6(20)	0(1)		1	1						x	x	3	
11.2–11.22		14(22)			0(1)		6(25)	0(2)		1				1			x	x	x	
12.0–12.02		6(34)		1	1(1)		5(15)					x				x	1	2		
13.25–13.27	1	7(32)	0(1)		0(1)		11(16)	1						1				x	x	
14.0–14.02		14(45)					0(5)			1				2			1			
15.2–15.22		11(40)	0(1)				1(6)	0(3)		1	1		x				x	x	x	
16.0–16.02		9(40)	0(1)				1(9)			1						x	x	x	x	
17.2–17.23		11(38)					6(11)	2(1)		x	x		x				x		x	
18.0–18.02		7(40)					1(10)			1							x			
19.2–19.23		5(44)					2(6)			2	3							x		
20.0–20.04		3(48)					0(2)							1					2	
21.2		2(15)	0(1)		0(1)		10(33)			1	1			x	x					
22.0–22.03	2	9(14)			1(2)		14(34)			1				2					1	
23.2–23.22		1(12)					8(38)							2			x		x	
24.0–24.04	x	3(15)					4(33)	0(2)		2		1	1							
25.2–25.22	x	5(35)		1			3(15)						x			x				
26.0–26.02		2(18)					12(32)			1				x						
27.18–27.22		1(5)			0(1)		10(44)						x							
28.0–28.02		2(24)	0(1)		3(4)		5(20)													
29.2–29.23	2	8(31)			1(3)		1(16)			2			x						1	
30.0–30.02		7(44)					0(6)			1				1			x			
31.2–31.23		0(8)			0(3)		5(38)		2	1				1				1		
32.0–32.02		2(16)	0(2)		1(4)		5(28)											2		
33.2–33.22		13(49)					0(1)			1								x		
34.0–34.02		21(47)			0(1)	1(2)		1	2	1			2							
35.2–35.22	1	7(18)			2(2)	0(1)	8(29)			2	x							x		
36.0–36.02		14(42)			1		2(8)			1				2					1	
37.2–37.22		1(8)	0(1)		1(4)	0(1)	5(38)												1	
38.0–38.02	x	5(32)			2(4)		3(14)							2					5	
39.2–39.22	1	2(8)	0(2)				6(40)			2	x		x							
40.0–40.02	x	0(7)	0(1)		3(8)		2(33)		0(1)	3			1			1	x	2		
41.0–41.02	1	4(12)	1(5)		0(3)		4(30)	0(2)					1	x			x		x	
42.0–42.02	1	1(19)	0(2)		1(2)		10(27)						1	1					3	
43.0–43.02	x	0(14)			0(6)		3(30)			1			x	x	x		x		x	
44.0–44.02		4(18)			2(2)	0(1)	4(29)												1	
45.0–45.02	1	0(8)			1(5)		1(37)			1				1				x		
46.0–46.02	x	3(35)	0(1)		0(5)	0(1)	2							1	x	x			2	
47.0–47.02		3(7)	0(1)		0(2)		4			1				x					1	
48.0–48.02	1	2(44)	1				3(6)			1				3					1	
49.0–49.02	x	0(28)			0(4)		1(18)			1				1				x		
50.0–50.02		3(46)	0(2)				0(2)							1	x	x			1	
51.0–51.02		0(44)	0(2)		1(1)		0(3)							x					1	
52.0–52.02		5(49)					1(1)							1	x				1	
53.0–53.02		1(44)			1(1)		2(5)						x							
54.0–54.02	x	1(42)					1(8)			1	x								1	
55.0–55.02		1(42)			2(2)		2(6)			1				1					x	
56.0–56.02		3(47)			0(1)		2(2)						x						x	
57.0–57.02		3(42)					0(8)		1				x	x	x			1		
58.0–58.02		1(45)		1	0(2)	2(3)							2					x		
59.0–59.02		0(47)			0(1)		1(2)						1			1		2		
60.0–60.02		6(47)					0(2)	0(1)		x	x		1	x				2		

Table 1: Continued. Part 4 from 6.

Depth (m)	<i>Hayella challengeri</i>	<i>Helicosphaera carteri</i>	<i>Helicosphaera euphratis</i>	<i>Helicosphaera granulata</i>	<i>Helicosphaera minuta</i>	<i>Helicosphaera vedderi</i>	<i>Helicosphaera walbersdorffensis</i>	<i>Helicosphaera wallichi</i>	<i>Helicosphaera</i> sp.	<i>Holodiscolithus macroporus</i>	<i>Iselithina fusa</i>	<i>Lithostromation perdurum</i>	<i>Micrantholithus articulatus</i>	<i>Micrantholithus flos</i>	<i>Micrantholithus vesper</i>	<i>Perforocalcinella fusiformis</i>	<i>Pontosphaera discopora</i>	<i>Pontosphaera japonica</i>	<i>Pontosphaera multipora</i>	<i>Pyrocyclus orangensis</i>
61.0–61.02	1	10(43)	0(1)				1(6)			x			x	x					1	
62.0–62.02		5(36)	1		2(2)		4(12)			2				1				1		
63.0–63.02		5(22)			1(4)		6(24)			1								4		
64.0–64.02		3(22)			1(2)		5(26)			1				1				1		
65.0–65.02	2	4(38)			3(2)		2(9)		0(1)	1					1	1			1	
66.0–66.02	2	7(38)			1(1)		6(11)			4		x						1		
67.0–67.02		5(34)			2(3)		2(13)			x	x							x		
68.0–68.02		7(37)	0(1)		0(2)		1(10)			1	x			1				x		
68.4–68.42		5(37)	0(1)		0(5)		4(7)							x	1			1		
69.0–69.02		7(34)			2(6)		2(10)					2		x				2		
70.0–70.02		3(43)			0(3)	1	0(4)			2				x				x		
71.0–71.02		5(47)			1		4(3)			1				x				2		
72.0–72.02		12(38)	0(1)		0(1)		3(10)			3				1				4		
73.0–73.02	1	14(28)	1(1)		0(2)		8(19)			x		x	1	x				1		
74.0–74.02		1(23)			3(14)		6(12)	0(1)		1				1						
75.0–75.02		10(19)			0(1)		12(30)							2				1		
76.0–76.02	x	6(34)			1		8(16)						1	x			4			
77.0–77.02		14(34)	0(1)		1		5(15)						x	x			3			
78.0–78.02	x	2(23)			1		2(27)			3		1	1				x			
79.0–79.02	x	2(13)			2(1)		7(36)						2	x			1	1		
80.0–80.02		5(22)					9(28)					1						2		
81.0–81.02	x	9(36)	0(1)		1(1)		1(11)	0(1)	1		x		x	2				1		
82.0–82.02	x	6(21)			1(1)	x	6(28)						1				1			
83.0–83.02	x	2(21)			0(2)		4(27)				1						1			
84.0–84.02	x	6(33)	x		3	1	2(17)						1				4			
84.8–84.82	x	4(24)	0(1)		3		4(25)						x				1			
85.0–85.02	1	2(9)			0(2)		4(39)			x			x					x		
86.0–86.02	1	4(13)					5(37)					1	1				3			
87.0–87.02	3	1(11)					11(39)					1	x			x	2			
88.0–88.02	2	1(17)			1		7(33)						x				x			
89.0–89.02	x	1(11)					1(39)			x		1					x			
90.0–90.02	3	0(1)			2(2)		14(47)							1						
91.0–91.02	1	1(3)			2(1)		10(46)			x			x	1	1			x		
92.0–92.02		3(8)			3(4)	0(2)	8(36)			1			1	2	x			1		
93.0–93.02	x	0(6)					8(44)			2	2	x	x					x		
94.0–94.02	1	4(6)	1				20(44)							1				1		
95.0–95.02	1	x			1		11(50)			x			x					x		
96.0–96.03		0(2)			0(3)		8(45)						x					x		
97.0–97.02		1(26)	x		0(1)		7(23)					1		1						
98.0–98.02		3(9)			1(2)		11(39)						1	1	1	2				
99.0–99.02		3(7)			1(3)		16(40)						x	1			1			
100.0–100.02		1(10)					15(40)	1		x			x					1		
100.4–100.42		1(3)			1(2)		24(45)						x					1		
100.6–100.62		1(1)			0(2)		16(47)						x				x		x	
100.8–100.83	x	3(2)	1		4(2)	1	49(46)					1	1				2			
101.0–101.02		0(3)			3(3)		25(44)		1	1			1				x		x	
101.2–101.22		1(1)			0(2)		26(47)			x			x				x		x	
101.6–101.62		2(5)			0(1)	x	11(44)			x			3		x	2				
101.8–101.82		2(3)			0(2)	x	15(45)		1				x					1		

Table 1. *Continued.* Part 5 from 6.

Table 1. Continued. Part 6 from 6.

Depth (m)	<i>Reticulofenestra gelida</i>	<i>Reticulofenestra haqii</i>	<i>Reticulofenestra minuta</i>	<i>Reticulofenestra pseudounbilicata</i> 5–7 µm	<i>Reticulofenestra pseudounbilicata</i> >7 µm	<i>Reticulofenestra sp.</i>	<i>Rhabdosphaera clavigera</i>	<i>Rhabdosphaera pannonica</i>	<i>Rhabdosphaera proceria</i>	<i>Rhabdosphaera sicca</i>	<i>Rhabdosphaera sp.</i>	<i>Sphenolithus abies</i>	<i>Sphenolithus heteromorphus</i>	<i>Sphenolithus milanetti</i>	<i>Sphenolithus moriformis</i>	<i>Sphenolithus sp.</i>	<i>Syracosphera pulchra</i>	<i>Thoracosphaera heimii</i>	<i>Thoracosphaera saxeae</i>	<i>Triquetorhabdulus challengerii</i>	<i>Triquetorhabdulus milowii</i>	<i>Umbilicosphaera jafarri</i>
61.0–61.02	3	30	184	54			2								1		1					9
62.0–62.02		28	179	19													1					58
63.0–63.02	1	18	172	26											1				x			29
64.0–64.02	2	19	169	30			7								2		x			x		51
65.0–65.02	2	19	173	15			8					x		1	1	x						50
66.0–66.02		11	140	25			2					1					1			x		99
67.0–67.02	1	18	154	29			4					1		x	x		x					64
68.0–68.02	4	29	171	28			2					4		1								43
68.4–68.42	1	30	221	36			1					4		1	x		2					28
69.0–69.02	3	17	252	26			11					2	1	1	1			1	x			7
70.0–70.02	2	23	161	37			2					x		2			2	x				66
71.0–71.02	3	21	185	46			1					x		2	3							6
72.0–72.02	5	19	182	58	x							2		1	4		1					22
73.0–73.02	1	14	158	60	x										x	x				1		14
74.0–74.02	2	28	161	40	x							x		1								23
75.0–75.02		23	182	28								1		x								39
76.0–76.02	1	15	216	17	x							1			2							32
77.0–77.02	13	35	177	36	1							2		3	1	2						18
78.0–78.02	6	5	229	37								x	1	x	1	2						11
79.0–79.02	2	21	184	23										1	2					x		35
80.0–80.02	6	36	265	14	1							1		3	1	1	1					11
81.0–81.02	3	18	221	28								1		3	1							15
82.0–82.02	2	18	229	12	1							2		2	4		1					28
83.0–83.02	1	23	223	15								1		4	x							36
84.0–84.02	2	15	269	12	1							1	1	3	1							21
84.8–84.82	1	19	240	5										1	1		x					25
85.0–85.02	7	75	205	2	x	1						x		1	3							26
86.0–86.02	3	38	190	10								x		1	6	1					x	26
87.0–87.02	7	36	180	8	1	1						x		3	1							22
88.0–88.02	2	45	190	4	3							2		5	1	1	1	x				8
89.0–89.02		12	295	11	5							3		3	1							1
90.0–90.02	1	65	235	15	2							3			x	1						10
91.0–91.02	1	22	288	25	7							x		x		1		1		1		13
92.0–92.02	2	54	205	18	4	1						1		4			1					17
93.0–93.02	1	19	225	14	3							x		7	2							2
94.0–94.02	14	38	167	26								1		x	1					x		8
95.0–95.02	1	12	256	12	x							x										9
96.0–96.03	1	24	296	21	3							x			x	2						4
97.0–97.02		21	235	16	x							1	1	x	x							
98.0–98.02	2	6	292	16								1		4	1	1						3
99.0–99.02	1	49	365	5								1		x	x	1			x			3
100.0–100.02		3	253	12								1		x	x		1					13
100.4–100.42		20	395	20								2					x					4
100.6–100.62	1	17	210	23										1			x					6
100.8–100.83	5	15	157	26	1							5		1	1	2						4
101.0–101.02	1	4	275	17								x		1	x							2
101.2–101.22	2	10	328	23	x							x				1	1	1				4
101.6–101.62	3	36	197	19								x	1	x	x						1	3
101.8–101.82	2	32	203	20								x		2	x	2	x					3

Table 2: Reworked calcareous nannoplankton from the Baden-Sooss core. Part 1 from 3.

Table 2: *Continued.* Part 2 from 3.

Table 2: *Continued.* Part 3 from 3.